The effective viscosity of a channel-type porous medium.

W.-P. Breugem[1]

Accepted for publication in Physics of Fluids, Sep 2007

[1] Royal Netherlands Meteorological Institute (KNMI), PO Box 201, 3730 AE De Bilt, The Netherlands

Abstract

An expression for the effective viscosity (μ_e) of a homogeneous channel-type porous medium has been derived by matching the Brinkman solution for the macroscopic flow with the volume average of the corresponding Stokes solution for the microscopic flow. In a least square error sense, the optimal value for μ_e is equal to $\mu(\epsilon - 3/7)/2$ for $\epsilon \geq 3/7$ and 0 for $\epsilon < 3/7$, where ϵ is the porosity and μ is the fluid viscosity. Thus $\mu_e < \mu$ for all ϵ. For $\mu_e = 0$ the Brinkman equation reduces to Darcy's law.

1 Introduction

Because of their complexity, flows through porous media are usually described in terms of macroscopic quantities. The macroscopic flow can be defined as the local volume–average of the microscopic flow through the pores. For sufficiently slow flow, i.e. when inertial effects are negligible, the macroscopic flow can be described by the semi-empirical Brinkman equation [1]:

$$0 \;=\; -\nabla\langle p\rangle^s + \mu_e\nabla^2\langle \mathbf{u}\rangle^s - \mu\,\epsilon\,\mathbf{K}^{-1}\cdot\langle \mathbf{u}\rangle^s, \tag{1}$$

where p is the pressure, $\mathbf{u}$ is the velocity, μ is the fluid viscosity, μ_e is the effective (or sometimes called 'apparent') viscosity, ϵ is the porosity, and $\mathbf{K}$ is the permeability tensor of the porous medium. The brackets $\langle..\rangle^s$ denote the volume average of the corresponding microscopic flow variable.

In order to solve the Brinkman equation, knowledge is required of ϵ, $\mathbf{K}$ and μ_e. For a highly porous medium composed of spheres, Brinkman [1] suggested that μ_e can be approximated by Einstein's formula [2],[3]:

$$\frac{\mu_e}{\mu} = 1 + \frac{5}{2}\left(1-\epsilon\right). \tag{2}$$

In his analysis Einstein considered spheres moving with the ambient fluid, which is different from the case of flow along spheres that stay at rest. It is not trivial that the effective viscosity in the latter case can be described by the same formula, though it should be correct in case of a strongly non-uniform flow, i.e. in the limit that the third term on the right-hand side of equation (1) is negligible compared to the second term. Later studies by Lundgren [4], Freed & Muthukumar [5] and Kim & Russel [6] confirmed the validity of equation (2) for a highly porous medium consisting of spheres.

Einstein's formula is valid only for ϵ close to unity. While in this case $\mu_e > \mu$, Brinkman [1] suspected that $\mu_e < \mu$ for lower porosities. By lack of knowledge about the precise dependence of μ_e from ϵ at lower porosities, he therefore simply approximated μ_e by μ. This approximation is still common practice in many studies of flows through porous media.

Most studies on the effective viscosity of porous media concerned porous media composed of spheres [4],[5],[6],[7],[8], or two-dimensional arrays of circular or ellipsoidal cylinders [9],[10],[11]. These studies indicated that the effective viscosity may be smaller or larger than the fluid viscosity, dependent of the porosity and the type of porous medium. Givler & Altobelli [12] determined the effective viscosity of a porous medium experimentally. For a porous medium composed of open-cell foam with a porosity of 0.972, they reported that the effective viscosity is 7.5 times the fluid viscosity, much higher than what may be expected from equation (2).

The effective viscosity of one class of porous media has not been investigated so far, namely that of channel-type porous media. Examples of this type are fractured rocks [13]. In an earlier study [14],[15] laminar flow was examined over and through a three-dimensional regular array of cubes with a porosity of 0.875. The flow in between the cubes bore resemblance with plane Poiseuille flow and this porous medium can therefore be classified as a channel-type porous medium. This study indicated that the effective viscosity of the array of cubes is lower than the fluid viscosity, though no attempt was made to calculate it quantitatively [15] (paragraph 4.6). This finding has motivated the present study. The main aim is to obtain an estimation of the effective viscosity of the simple channel-type porous medium sketched in figure 1. The second aim is to quantify the improved accuracy of the solution of the Brinkman equation (1) when using this estimate of the effective viscosity compared to the commonly used assumption that $\mu_e = \mu$.

The structure of this paper is as follows. In section 2 it is shown that the Brinkman equation contains an implicit closure model for the drag force that a porous medium exerts on the macroscopic flow. This closure model is used in section 3 to derive an expression for the effective viscosity in case of a weakly non-uniform flow characterized by an infinitely small, but non-zero, wavenumber. In section 4 the improved accuracy of the Brinkman solution over a wide range of wavenumbers and porosities is quantified numerically for this estimate of μ_e compared to the common assumption that $\mu_e = \mu$. This is followed by a summary of the conclusions and a discussion in section 5.

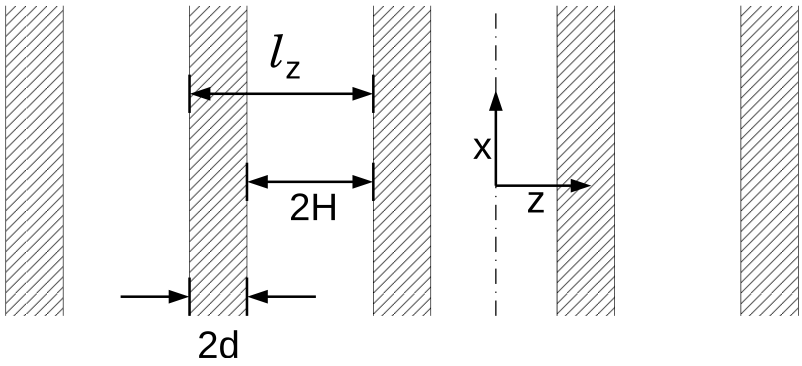

Figure 1: A simple spatially periodic two-dimensional channel-type porous medium.

2 Brinkman closure model for drag force

The macroscopic velocity through a porous medium can be formally defined as a local weighted volume–average of the microscopic velocity. This can be expressed mathematically by [16]:

$$\langle \mathbf{u} \rangle^s \equiv \int_V \gamma(\mathbf{x}+\mathbf{x}')\, m(\mathbf{x}')\, \mathbf{u}(\mathbf{x}+\mathbf{x}')\, d\mathbf{x}'. \tag{3}$$

Here $\mathbf{x}'$ is the position vector relative to the centroid $\mathbf{x}$ of the averaging volume V, γ is the phase–indicator function equal to 1 in the fluid phase and to 0 in the solid phase, and m is the filter or weighting function that is normalized such that its integral over V equals unity. The volume average defined by equation (3) is usually referred to as the *superficial* volume average, hence the superscript s. Sometimes it is convenient to make use of the *intrinsic* volume average, defined as $\langle \mathbf{u} \rangle \equiv \langle \mathbf{u} \rangle^s/\epsilon$, where $\epsilon \equiv \langle 1 \rangle^s$ is the porosity of the porous medium.

The microscopic velocity $\mathbf{u}$ can be decomposed into the macroscopic velocity $\langle \mathbf{u} \rangle$ and the subfilter-scale velocity $\tilde{\mathbf{u}}$ according [17]:

$$\mathbf{u} = \langle \mathbf{u} \rangle + \tilde{\mathbf{u}}. \tag{4}$$

Ideally, for meaningful volume averages, the macroscopic velocity should vary on much larger scales than the subfilter-scale velocity. In addition, the filter length l_f should be chosen such that in the volume averaging the macro-scale structure of $\mathbf{u}$ is preserved as much as possible, while the strongly inhomogeneous pore-scale structure of $\mathbf{u}$ is averaged out. With respect to this it can be expected that some filters perform better than others. This problem has been thoroughly investigated by Quintard & Whitaker [16]. They made distinction between ordered and disordered porous media, for which appropriate filters were proposed and validated. For the two types of porous media the above constraints can be summarized as:

$$\text{ordered} \;:\; O(l_p) = l_f \ll L_m, \tag{5a}$$

$$\text{disordered} \;:\; l_p \ll l_f \ll L_m, \tag{5b}$$

where l_p and L_m are the typical length scales of the pore-scale and the macro-scale flow field, respectively. When these constraints are satisfied, volume averages are *well-behaved* with $\langle\langle \mathbf{u} \rangle\rangle \approx \langle \mathbf{u} \rangle$ and $\langle \tilde{\mathbf{u}} \rangle \approx \mathbf{0}$ [17].

At the microscopic level, slow flow through a porous medium is governed by the incompressible Stokes equations:

$$0 = -\nabla p + \mu \nabla^2 \mathbf{u}, \tag{6a}$$

$$\nabla \cdot \mathbf{u} = 0. \tag{6b}$$

The macroscopic counterparts of these equations are found by application of the volume–averaging operator $\langle .. \rangle^s$. The results read [16]:

$$0 = -\nabla \langle p \rangle^s + \mu \nabla^2 \langle \mathbf{u} \rangle^s + \int_{A_i} m\, \mathbf{n} \cdot [-p\mathbf{I} + \mu\, \nabla \mathbf{u}]\ dA, \tag{7a}$$

$$\nabla \cdot \langle \mathbf{u} \rangle^s = 0. \tag{7b}$$

Here the surface integral extends over the interface area A_i between the fluid and solid phase within the averaging volume V, $\mathbf{n}$ is the unit normal at A_i pointing from the fluid into the solid phase, and $\mathbf{I}$ is the unit tensor. The last term in equation (7a) represents the drag force exerted by the solid phase onto the fluid phase within the averaging volume V.

Equation (7a) is exact, but for solving it a closure is needed for the surface integral in terms of volume-averaged quantities. A complication is its *non-local* character [16], since volume averages appear inside the surface integral when p and $\mathbf{u}$ are decomposed according to equation (4). However, by choosing an appropriate filter Quintard & Whitaker [16] showed that for *ordered* porous media the volume averages can be removed from the surface integral:

$$0 = -\nabla \langle p \rangle^s + \mu \nabla^2 \langle \mathbf{u} \rangle^s + \int_{A_i} m\, \mathbf{n} \cdot [-\tilde{p}\mathbf{I} + \mu\, \nabla \tilde{\mathbf{u}}]\ dA \tag{8}$$

For *disordered* homogeneous porous media this simplifiction holds by good approximation when condition (5b) is satisfied.

The Brinkman equation (1) is an approximation of equation (8). From equation (8) the Brinkman equation is obtained when the following closure model for the drag force is adopted:

$$\int_{A_i} m\, \mathbf{n} \cdot [-\tilde{p}\mathbf{I} + \mu\, \nabla \tilde{\mathbf{u}}]\ dA \approx -\mu\, \epsilon\, \mathbf{K}^{-1} \cdot \langle \mathbf{u} \rangle^s + (\mu_e - \mu)\, \nabla^2 \langle \mathbf{u} \rangle^s. \tag{9}$$

The second term on the right–hand side of equation (9) should not be confused with diffusion effects by mechanical and/or turbulent dispersion [18]. It can be interpreted as the porous media analogue of the Faxén correction [19] to Stokes's drag law for flow around a sphere. Since this correction term is proportional to the Laplacian of the velocity, it appears as a modification of the fluid viscosity in the Brinkman equation (1).

Lundgren [4], Freed & Muthukumar [5], Kim & Russel [6] and Koplik, Levine & Zee [7] gave theoretical support for the validity of the Brinkman closure model (9) for porous media composed of randomly distributed spheres. Kim & Russel [6] (KR for short) argued that for this disordered porous medium the Brinkman equation holds only when the particle volume fraction $c\,(= 1 - \epsilon)$ is small, based on similar constraints as given by equation (5b). Equivalent to $l_p \ll l_f$, they demanded that the averaging volume contains many particles. This can be expressed as $c(l_f/a)^3 \gg 1$, where a is the radius of the spherical particles. Furthermore, equivalent to $l_f \ll L_m$, they demanded that the dimension of the averaging volume is small compared to the scales of the volume-averaged flow field. KR took $L_m = O(\sqrt{K})$ based on considering the variations in $\langle p\rangle^s$ in the hypothetical case that $\nabla\langle \mathbf{u}\rangle^s$ would be spatially uniform. Combining the two constraints together, it follows that $c^{1/3}\sqrt{K}/a \gg 1$, which can be satisfied only for $c \ll 1$ as in this limit $\sqrt{K}/a = O(c^{-1/2})$.

Note that for obtaining the second constraint, KR considered the specific flow case of a uniform $\nabla\langle \mathbf{u}\rangle^s$ for which, according to the Brinkman equation (1), a *strongly non-uniform* $\langle p\rangle^s$ is needed to maintain this. This resulted in the estimate $L_m = O(\sqrt{K})$, which is however not generally true for other flow cases. A more general case would be to consider a non-uniform macroscopic flow that varies in space at a typical wavenumber k, so that $L_m = O(2\pi/k)$. Combining this with $c(l_f/a)^3 \gg 1$, this yields $(ka/2\pi)^3 \ll c \leq 1$. This condition states that the Brinkman equation is valid for all c provided that for given c the wavenumber k is sufficiently small, while the original KR condition suggests that it is valid only for small c.

In this paper we consider flow through the channel-type porous medium of figure 1, which is driven by a streamwise pressure gradient that varies sinusoidally across the channels at wavenumber k. Thus $L_m = O(2\pi/k)$. Furthermore, for this ordered porous medium the filter length is equal to the dimension l_z of the unit cell (see next section). The constraint (5a) becomes thus that $kl_z/2\pi \ll 1$, which is independent of the porosity.

The Brinkman closure model (9) for the drag force is used in the next section to derive an expression for the effective viscosity. Because of the constraint that the wavenumber must be sufficiently small, the expression for the effective viscosity is derived for the limit of an infinitely small, but still non–zero, wavenumber.

3 Estimate of effective viscosity

We consider an arbitrary non-uniform streamwise pressure gradient that varies periodically across the height of the channels in figure 1. A spatially periodic pressure gradient can be expressed in a Fourier series. Since the Stokes equation (6a) is linear, we may restrict ourselves to a single cosine function without loss of generality:

$$-\frac{\partial p}{\partial x} = A\cos(kz), \tag{10}$$

where A is the amplitude and k is the wave number. The corresponding velocity field in the channels can be computed from the Stokes equation (6a) and the no-slip condition at the channel walls. For $|z| \in [0, 3H + 2d]$ the solution reads:

$$u(z) = \left\{ \begin{array}{ll} A\left[\cos(kz) - \cos(kH)\right]/(\mu k^2) & , |z| \in [0, H] \ , \\ A\cos(kz)/(\mu k^2) + C_1 z + C_2 & , |z| \in [H + 2d, 3H + 2d] \ , \end{array} \right. \tag{11}$$

with the coefficients C_1 and C_2 given by:

$$\begin{aligned} C_1 &= \frac{A}{\mu k^2 2H}\Big(\cos(k[H + 2d]) - \cos(k[3H + 2d])\Big) \,, \\ C_2 &= -\frac{A(3H + 2d)}{\mu k^2 2H}\cos(k[H + 2d]) + \frac{A(H + 2d)}{\mu k^2 2H}\cos(k[3H + 2d]). \end{aligned}$$

To compute the macroscopic flow field from equation (3), we need to choose an appropriate weighting function. For spatially periodic porous media Quintard & Whitaker [16] proposed the following triangular-shaped weighting function:

$$m(z') = \left\{ \begin{array}{ll} (l_z - |z'|)/l_z^2 & , |z'| \le l_z \ , \\ 0 & , |z'| > l_z \ , \end{array} \right. \tag{12}$$

where $l_z = 2(H+d)$ is the size of a unit cell in the z-direction. It is precisely this weighting function for which equation (8) is exact. Using this weighting function the volume-averaged velocity for $|z| \in [0, H]$ is given by:

$$\begin{aligned} \langle u \rangle^s &= -\frac{1}{\mu k^2}\frac{\partial \langle p \rangle^s}{\partial x} + \frac{2A\sin^2(kl_z/2)}{\mu k^2 l_z^2}\cos(kH)\left(z^2 + H^2\right) \\ &\quad -\frac{\epsilon A\cos(kH)}{\mu k^2} - \frac{\epsilon^2 A}{6\mu k^2}\sin(kl_z)\sin(kH), \end{aligned} \tag{13a}$$

with the gradient of the volume-averaged pressure given by:

$$\begin{aligned} -\frac{\partial \langle p \rangle^s}{\partial x} &= \frac{4A\sin(kl_z/2)}{k^2 l_z^2}\Big[\sin(kl_z/2)\cos(kz) - \sin(kd) \ - kH\cos(kd)\Big] + \\ &\quad \frac{2A}{kl_z}\sin(kH). \end{aligned} \tag{13b}$$

Over the same interval, the following expressions are obtained for the diffusion term and the drag force in equation (8):

$$\mu\frac{\partial^2 \langle u \rangle^s}{\partial z^2} = \frac{4A\sin^2(kl_z/2)}{k^2 l_z^2}\Big[-\cos(kz) + \cos(kH)\Big] \,, \tag{13c}$$

$$\begin{aligned} \int_{A_i} m\, n_z\, \mu\frac{\partial \tilde{u}}{\partial z}\, dA &= \frac{4A\sin(kl_z/2)}{k^2 l_z^2}\Big[kH\cos(kd) - \ \sin(kH)\cos(kl_z/2)\Big] - \\ &\quad \frac{2A}{kl_z}\sin(kH). \end{aligned} \tag{13d}$$

For small values of k, equations (13a)-(13d) can be simplified according to:

$$\langle u\rangle^s = \frac{\epsilon A H^2}{3\mu} - \frac{A k^2 H^4}{24\mu}\left(\frac{4\epsilon}{15} + 3 + 6\left[\frac{z}{H}\right]^2 - \left[\frac{z}{H}\right]^4\right) + O(k^4), \quad (14a)$$

$$-\frac{\partial\langle p\rangle^s}{\partial x} = \epsilon A + \frac{A H^2 k^2}{2}\left(-\left[\frac{z}{H}\right]^2 - 1 + \frac{\epsilon}{3}\right) + O(k^4), \quad (14b)$$

$$\mu\frac{\partial^2\langle u\rangle^s}{\partial z^2} = \frac{A H^2 k^2}{2}\left(\left[\frac{z}{H}\right]^2 - 1\right) + O(k^4), \quad (14c)$$

$$\int_{A_i} m\, n_z\, \mu\frac{\partial\tilde{u}}{\partial z}\, dA = -\epsilon A + \frac{A H^2 k^2}{2}\left(2 - \frac{\epsilon}{3}\right) + O(k^4). \quad (14d)$$

The permeability K_{xx} of the porous medium can now be calculated by taking the limit of $k \to 0$ and using equation (9):

$$K_{xx} = \lim_{k\to 0}\frac{-\mu\epsilon\langle u\rangle^s}{\int_{A_i} m\, n_z\, \mu\frac{\partial\tilde{u}}{\partial z}\, dA} = \frac{\epsilon H^2}{3}, \quad (15)$$

which is a well-known result [13].

Finally, an expression for the effective viscosity is found from the requirement that it minimizes the square residual error of the Brinkman closure model (9) on global average. For $z \in [0, H]$ the mean square residual error is given by:

$$\overline{R^2} = \frac{1}{H}\int_0^H \left(\int_{A_i} m\, n_z\, \mu\frac{\partial\tilde{u}}{\partial z}\, dA + \mu\frac{\epsilon}{K_{xx}}\langle u\rangle^s - (\mu_e - \mu)\frac{\partial^2\langle u\rangle^s}{\partial z^2}\right)^2 dz. \quad (16)$$

With help of equations (14a), (14d) and (15), and requiring that $\mu_e \geq 0$ for physically realistic Brinkman solutions, this yields the following estimate of μ_e valid for $k \ll 1$:

$$\frac{\mu_e}{\mu} \approx \begin{cases} 0 & , \epsilon \in [0, \frac{3}{7}) \ , \\ \frac{1}{2}\left(\epsilon - \frac{3}{7}\right) & , \epsilon \in [\frac{3}{7}, 1] \ . \end{cases} \quad (17)$$

The effective viscosity is always smaller than the fluid viscosity, consistent with the findings in [15] for a regular array of cubes. For $\epsilon \leq 3/7$, $\mu_e \approx 0$, in which case the Brinkman equation reduces to Darcy's law [13]. For $\epsilon \to 1$, neither the effective viscosity approaches the fluid viscosity μ, nor the permeability given by (15) becomes infinite. This originates from the no-slip condition at the channel walls, which must be satisfied even when the channel walls become infinitely thin for $\epsilon \to 1$.

To illustrate the accuracy of the effective viscosity estimate, we consider the case of $kl_z/2\pi = 0.233$ and $\epsilon = 0.5$. The Reynolds number $Re \equiv \rho u_\tau H/\mu = 0.1$, with ρ the fluid density and $u_\tau \equiv \sqrt{|\mu\partial u/\partial z|_{z=H}/\rho}$ the microscopic friction velocity at $z = H$. Figure 2.a shows the dimensionless microscopic and the corresponding volume-averaged flow field for $z/l_z \in [0, 10]$. Inside the channel walls the microscopic velocity is put to zero. Figure 2.b shows the different terms in the volume-averaged momentum budget (8). The pressure gradient is balanced mainly by the drag force. The effect of diffusion is small, though not

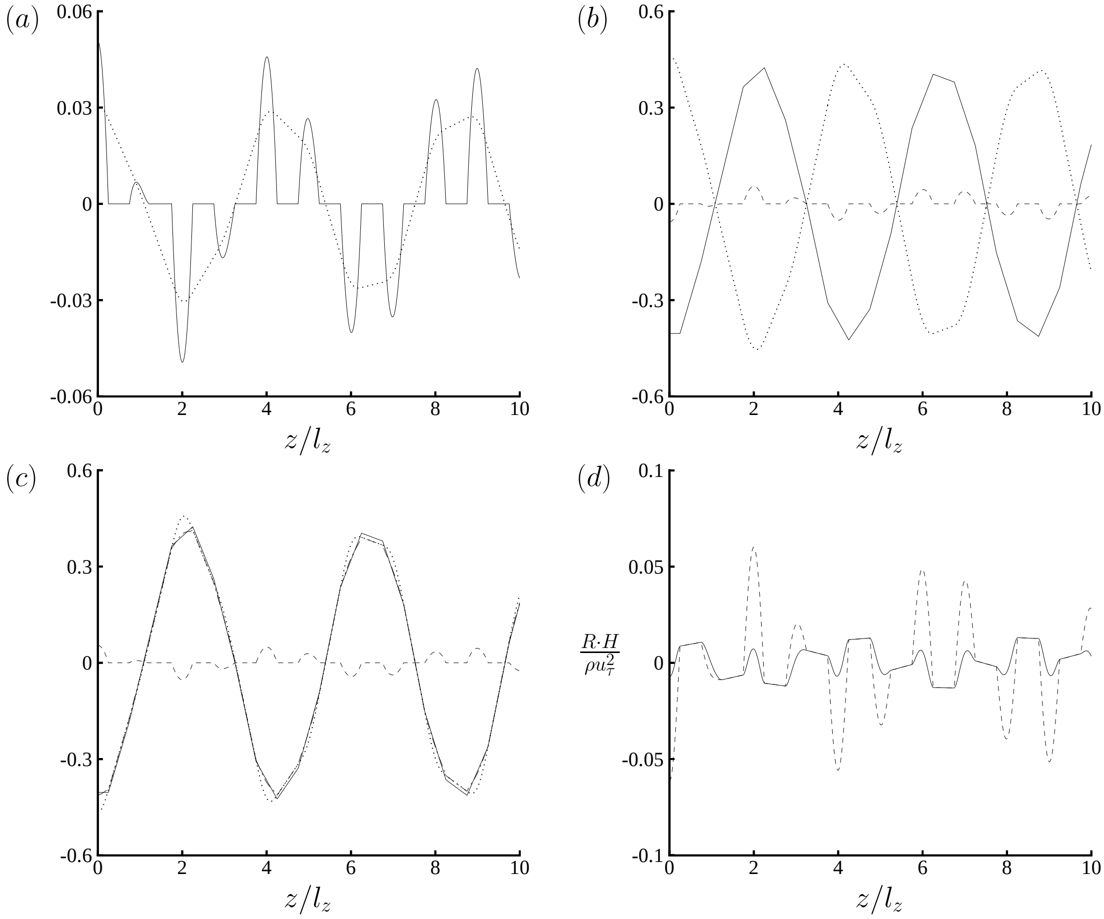

Figure 2: (a) Microscopic and volume-averaged velocity field for $kl_z/2\pi = 0.233$, $\epsilon = 0.5$ and $Re = 0.1$. ——, u/u_τ; $\cdots\cdots$, $\langle u\rangle/u_\tau$. (b) Corresponding volume-averaged momentum balance (8), normalized by $\rho u_\tau^2/H$. ——, $\int_{A_i} m\, n_z\, \mu \frac{\partial \tilde{u}}{\partial z} dz$; $\cdots\cdots$, $-\frac{\partial \langle p\rangle^s}{\partial x}$; $- - -$, $\mu \frac{\partial^2 \langle u\rangle^s}{\partial z^2}$. (c) Validation of Brinkman closure model (9) with $\mu_e = \mu(\epsilon - 3/7)/2$ and normalized by $\rho u_\tau^2/H$. ——, $\int_{A_i} m\, n_z\, \mu \frac{\partial \tilde{u}}{\partial z} dz$; $\cdots\cdots$, $-\mu \frac{\epsilon}{K_{xx}} \langle u\rangle^s$; $- - -$, $(\mu_e - \mu) \frac{\partial^2 \langle u\rangle^s}{\partial z^2}$; $- \cdot - \cdot -$, $-\mu \frac{\epsilon}{K_{xx}} \langle u\rangle^s + (\mu_e - \mu) \frac{\partial^2 \langle u\rangle^s}{\partial z^2}$. (d) Residual error ($R$) of Brinkman closure model (9) normalized by $\rho u_\tau^2/H$. Note that the vertical scaling is different from (c). ——, $\mu_e = \mu(\epsilon - 3/7)/2$; $- - -$, $\mu_e = \mu$.

negligible. Figure 2.c depicts the different terms in the Brinkman closure model (9) with $\mu_e = \mu(\epsilon - 3/7)/2$. The lion's share of the drag force is accounted for by the first term on the right-hand side of (9), but this term generally overestimates the drag. The second term on the right-hand side of (9) compensates for this and significantly improves the estimate of the drag; the dash-dotted line collapses almost entirely with the solid line. The residual error of (9) is plotted in figure 2.d for $\mu_e = \mu(\epsilon - 3/7)/2$ compared to the commonly used assumption that $\mu_e = \mu$. Although the local error for $\mu_e = \mu(\epsilon - 3/7)/2$ is sometimes slightly larger than for $\mu_e = \mu$, the global error is much smaller, confirming the improved accuracy of the Brinkman closure model for this estimate of μ_e with respect to $\mu_e = \mu$.

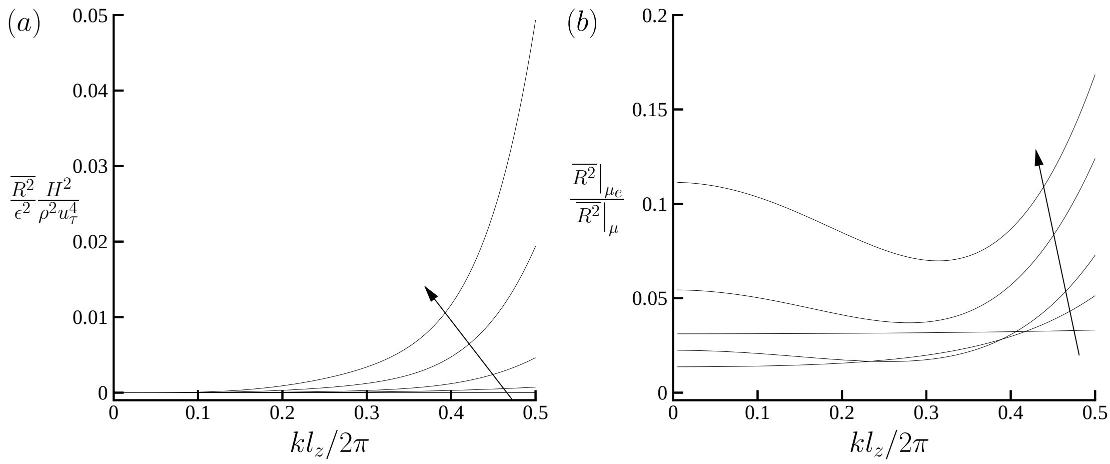

Figure 3: (a) $\overline{R^2}$, as given by equation (16) and normalized by $\epsilon^2\rho^2 u_\tau^4/H^2$, as function of wavenumber and porosity for μ_e given by equation (17). (b) Ratio of $\overline{R^2}$ for μ_e given by (17) to $\overline{R^2}$ for $\mu_e = \mu$. The arrows point in the direction of increasing porosity with $\epsilon = 0.01, 0.25, 0.5, 0.75, 0.99$.

To further test the accuracy of the estimate for the effective viscosity, $\overline{R^2}$ has been calculated over a wide range of k and for different porosities with help of equations (13a), (13d) and (15). For a honest comparison of $\overline{R^2}$ at different porosities, its intrinsic form must be considered, and it is therefore divided by ϵ^2. It is furthermore nondimensionalized by $\rho^2 u_\tau^4/H^2$. The absolute error is depicted in figure 3.a and the relative error compared to the case that $\mu_e = \mu$ in figure 3.b. The absolute error increases for larger ϵ and larger k. The latter is consistent with the condition derived in the previous section that the Brinkman equation is valid for $kl_z/2\pi \ll 1$. The relative error has a more complex behavior as function of k and ϵ. According to figure 3.b, the largest mean square residual error, for $\epsilon \to 1$, is still typically an order of magnitude smaller for μ_e given by equation (17) as compared to the case that μ_e is simply taken equal to μ.

4 Error estimate of Brinkman solution

In this section the error in the solution of the Brinkman equation (1) is quantified numerically for μ_e given by (17) compared to the commonly used assumption that $\mu_e = \mu$. This is done by comparing the numerical solution of the Brinkman equation for the channel-type porous medium of figure 1 against the volume average of the corresponding solution of the Stokes equation. We will first briefly discuss the two types of simulations before we move on to the results.

In the simulations of the microscopic flow the instationary Stokes equation was solved, i.e. equation (6a) with the temporal derivative of the velocity on the left-hand side. The flow was forced by the pressure gradient given by equation (10) with the wavenumber in the range of $2\pi k/l_f \in [0, 0.5]$. The Reynolds number was fixed at $Re = 0.1$. The flow domain extended from $z = 0$ to $z = 12l_f + H$. The boundary conditions were the no-slip condition at the channel walls and the free-slip condition at $z = 0$. The instationary Stokes equation was discretised on a uniform grid with the grid spacing $\Delta z = H/80$. Spatial derivatives were approximated with the central differencing scheme. For the integration in time the second-order Adams-Bashforth scheme [20] was used, with the time step equal to $\Delta t = \rho \Delta z^2/(24\mu)$. A stationary solution was typically obtained after a time of $0.3H/u_\tau$. The volume-averaged velocity was subsequently computed from equation (3) using the weighting function given by equation (12).

In the simulations of the macroscopic flow the Brinkman equation was solved. The pressure gradient in this equation was obtained from volume averaging of the microscopic pressure gradient, which for $z \in [0, H]$ is given by equation (13b). The Reynolds number for the macroscopic flow was the same as for the microscopic flow, while the flow domain was slightly smaller, extending from $z = 0$ to $z = 11l_f + H$. The Brinkman equation was discretised on a uniform grid with the same grid spacing as used for the microscopic flow. The boundary conditions were the free-slip condition at $z = 0$ and $\langle u \rangle^s$ equal to the volume average of the microscopic solution at $z = 11l_f + H$. Different from the microscopic flow domain, the macroscopic flow domain contained no internal boundaries, so the discretised Brinkman equation could be written as a linear matrix system of form $MU = G$, with M a tridiagonal matrix, and U and G the grid representation vectors of the volume-averaged velocity and the pressure gradient, respectively. The volume-averaged flow field was obtained from this system by means of Gauss elimination [20]. Two solutions were computed from the Brinkman equation. The first one corresponded to $\mu_e = \mu$ and the second one to μ_e given by equation (17).

As an example figure 4 depicts the volume average of the microscopic solution and the two macroscopic solutions (for $\mu_e = \mu$ and $\mu_e = \mu(\epsilon - 3/7)/2$) for $\epsilon = 0.5$ and $kl_z/2\pi = 0.233$. The Brinkman solution for $\mu_e = \mu$ may deviate locally less from the volume average of the microscopic solution than the Brinkman solution for $\mu_e = \mu\,(\epsilon - 3/7)/2$, but over most of the flow domain the deviation is significantly smaller in the latter case. The

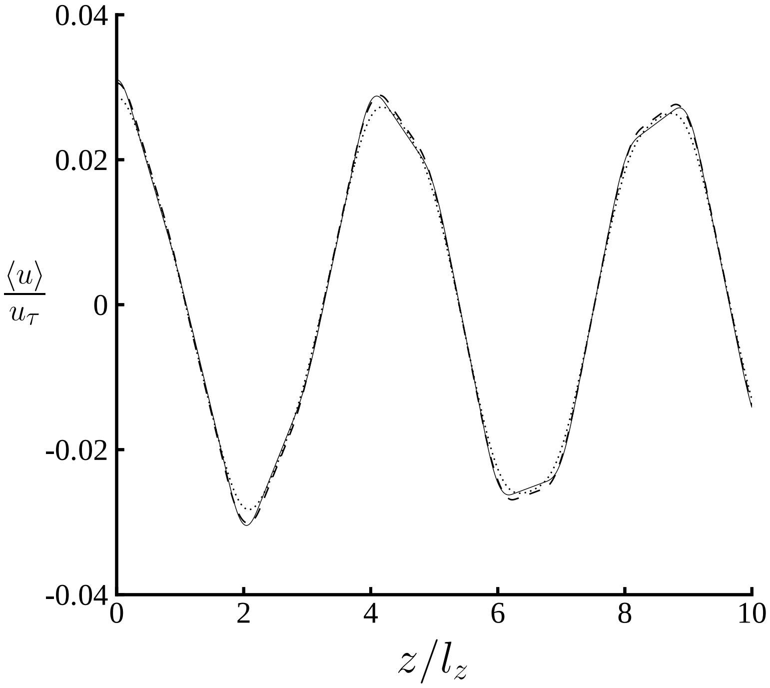

Figure 4: Volume-averaged flow field for $kl_z/2\pi = 0.233$, $\epsilon = 0.5$ and $Re = 0.1$. ——, $\langle u \rangle / u_\tau$ computed from microscopic flow field; $\cdot\cdot\cdot\cdot\cdot$, $\langle u \rangle / u_\tau$ computed from Brinkman equation with $\mu_e = \mu$; $- - -$, $\langle u \rangle / u_\tau$ computed from Brinkman equation with $\mu_e = \mu\,(\epsilon - 3/7)/2$.

deviations have been quantified by computing the mean square error from:

$$\overline{E^2} = \frac{1}{10 l_f} \int_0^{10 l_f} \left[\langle u \rangle_{bs} - \langle u \rangle_{ms} \right]^2 dz, \tag{18}$$

where the subscripts bs and ms denote the Brinkman solution and the volume average of the microscopic solution, respectively. Figure 5.a shows $\overline{E^2}$ for μ_e given by (17) as function of wavenumber and porosity. The smaller the wavenumber and the porosity, the smaller the error. The waviness in the profiles at larger wavenumber is due to the relatively short domain size; the waviness becomes smaller when the domain size is increased. Figure 5.b shows the relative error, defined as the ratio of $\overline{E^2}$ for μ_e given by (17) to $\overline{E^2}$ for $\mu_e = \mu$. In the limit of $k \to 0$, when diffusion becomes negligible, the relative error reaches 1. For small, but non-zero, wavenumber the relative error rapidly decreases, while for larger wavenumber it goes up again. The results show that over a large range of wavenumbers the error is an order of magnitude smaller when μ_e is given by (17) as compared to $\mu_e = \mu$.

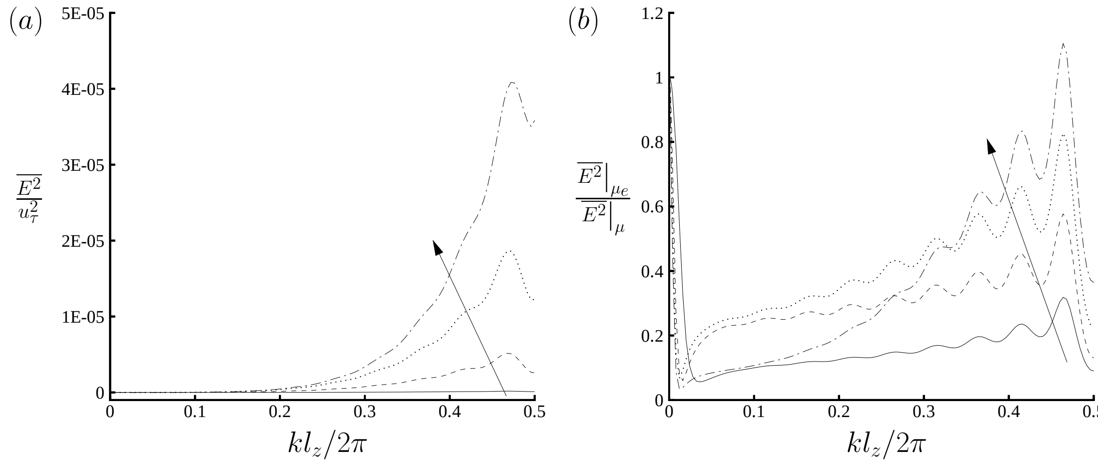

Figure 5: (a) $\overline{E^2}$ calculated from equation (18) and normalized by u_τ^2, as function of wavenumber and porosity for μ_e given by (17). (b) Ratio of $\overline{E^2}$ for μ_e given by (17) to $\overline{E^2}$ for $\mu_e = \mu$. The arrows point in the direction of increasing porosity. ——, $\epsilon = 0.2$; $- - -$, $\epsilon = 0.5$; $\cdots\cdots$, $\epsilon = 0.73$; $\cdot - \cdot - \cdot - \cdot$, $\epsilon = 0.99$.

5 Conclusions and discussion

The effective viscosity of a simple channel-type porous medium has been derived by matching the macroscopic Brinkman solution to the volume average of the Stokes solution for the microscopic flow. The optimal value for μ_e is given by equation (17). For all ϵ, $\mu_e < \mu$. For $\epsilon \leq 3/7$, $\mu_e = 0$, and the Brinkman equation reduces to Darcy's Law. A quantitative error estimate confirmed the improved accuracy of the Brinkman solution based on μ_e given by (17) as compared to the commonly used assumption that $\mu_e = \mu$; at all porosities the global error is typically an order of magnitude smaller over a large range of wavenumbers. The absolute error in the Brinkman solution becomes large near $kl_z/2\pi = O(1)$, which substantiates the theoretically derived condition that the Brinkman equation is valid only for sufficiently small wavenumbers.

The effective viscosity is not only a function of the porosity, but, as mentioned in the introduction, it also strongly depends on the geometrical structure of a porous medium. With respect to this porous media can be divided into three different types dependent of the structure of the pore-scale flow field [21]: the channel (or conduit) type, the bluff-body type, and the more general hybrid type that bears characteristics of both other types. In the channel type the (Stokes) flow is aligned along the surface of the solid elements and consequently the drag is purely viscous drag, while for the bluff-body type the flow is generally not aligned along the solid elements and hence both viscous and pressure drag contribute to the total drag. The present paper is the first in which μ_e is thoroughly evaluated for a channel-type porous medium. For this type the behavior of μ_e at high porosities is completely different from the bluff-body type such as for instance a random array of spheres. While for the channel-type porous medium $\mu_e < \mu$, for the random array of spheres $\mu_e > \mu$ according to equation (2).

In the derivation of the effective viscosity we made use of the triangular-shaped filter as given by equation (12). Another well-known weighting function is the rectangular-shaped filter given by equation (A-1) in the appendix. It is shown in the appendix that for homogeneous porous media the estimate of μ_e would be the same for both filters if the drag closure (9) would be exact. In general this is not true. However, one may expect that the residual (R) is usually small compared to the second term on the right-hand side of equation (9), as for instance can be observed from figures 2.c,d. In that case the effective viscosity estimate is insensitive to the choice of the filter and the interval over which $\overline{R^2}$ is minimized.

The analysis in this paper was restricted to a homogeneous porous medium, i.e. a porous medium with a spatially uniform porosity. Porous media generally become heterogeneous near macroscopic boundaries, such as for instance the interface between a porous medium and a clear fluid or a macroscopic solid wall. The present analysis could be extended by considering the effect of spatial heterogeneity of a porous medium on the effective viscosity. Is the local effective viscosity of a (weakly) heterogeneous porous medium solely a function of the local porosity? If this is the case, does this mean that the effective viscosity can then be determined from an analysis of the corresponding homogeneous porous medium with the same porosity? This issue may not be easy to analyze analytically, but it could be investigated with help of detailed numerical simulations of microscopic Stokes flow through heterogeneous porous media. Several numerical methods are available for this kind of simulations such as the Lattice Boltzmann Method [22] and the Immersed Boundary Method [23]. The Immersed Boundary Method has been successfully used in previous studies of the author to simulate both laminar and turbulent flows over and through a three-dimensional array of cubes [14],[15],[24],[25].

Acknowledgments

The author would like to thank Prof. B. J. Boersma for his comments to improve the manuscript.

Appendix A: Effect filter on effective viscosity estimate

In this paper we made use of the triangular-shaped filter (12). Another well-known filter is the following rectangular-shaped filter:

$$m(z') = \begin{cases} 1/l_z & , |z'| \leq l_z/2 \ , \\ 0 & , |z'| > l_z/2 \ . \end{cases} \tag{A-1}$$

Recall that l_z is the size of a unit cell in the z-direction. Both filters have been discussed by Quintard & Whitaker [16]. It can be shown that the application of the triangular-shaped filter is equivalent to twice the application of the rectangular-shaped filter:

$$\langle u \rangle_t^s = \frac{1}{l_z^2} \int_{-l_z/2}^{l_z/2} \int_{-l_z/2}^{l_z/2} \gamma(z + z' + \hat{z}) u(z + z' + \hat{z}) \; d\hat{z} dz' = \langle \langle u \rangle_r^s \rangle_r, \tag{A-2}$$

where the subscripts t and r refer to, respectively, the triangular-shaped and the rectangular-shaped filter. Below we analyze the effect of the filter choice on the estimate of the effective viscosity.

Let us consider Stokes flow through a homogeneous porous medium with the volume-averaged flow directed along the x-axis. Application of the rectangular-shaped filter to the streamwise component of the Stokes equation (6a) yields:

$$0 = -\frac{\partial \langle p \rangle_r^s}{\partial x} + \mu_{e,r} \frac{\partial^2 \langle u \rangle_r^s}{\partial z^2} - \mu \frac{\epsilon_r}{K_{xx,r}} \langle u \rangle_r^s + R_r. \tag{A-3}$$

Here R_r is the residual at the right-hand side of equation (9); $R_r = 0$ if the drag closure would be exact. Once more applying the rectangular-shaped filter to equation (A-3) yields:

$$0 = -\frac{\partial \langle \langle p \rangle_r^s \rangle_r}{\partial x} + \mu_{e,r} \frac{\partial^2 \langle \langle u \rangle_r^s \rangle_r}{\partial z^2} - \mu \frac{\epsilon_r}{K_{xx,r}} \langle \langle u \rangle_r^s \rangle_r + \langle R_r \rangle_r. \tag{A-4}$$

Direct application of the triangular-shaped filter to the Stokes equation yields:

$$0 = -\frac{\partial \langle \langle p \rangle_r^s \rangle_r}{\partial x} + \mu_{e,t} \frac{\partial^2 \langle \langle u \rangle_r^s \rangle_r}{\partial z^2} - \mu \frac{\epsilon_t}{K_{xx,t}} \langle \langle u \rangle_r^s \rangle_r + R_t. \tag{A-5}$$

It is not difficult to show that for a homogeneous porous medium, for which the porosity and permeability are spatially uniform, $\epsilon_t = \epsilon_r$ and $K_{xx,t} = K_{xx,r}$. But are the effective viscosities, $\mu_{e,t}$ and $\mu_{e,r}$, also the same? Subtracting equations (A-4) and (A-5) from each other gives:

$$0 = (\mu_{e,t} - \mu_{e,r}) \frac{\partial^2 \langle \langle u \rangle_r^s \rangle_r}{\partial z^2} + R_t - \langle R_r \rangle_r. \tag{A-6}$$

For the moment let us assume that $\mu_{e,t} = \mu_{e,r}$. Then from (A-6) it must follow that $R_t = \langle R_r \rangle_r$. In this paper the effective viscosity has been determined from minimizing the mean square residual error at low wavenumber over a specified spatial interval. In case of the triangular-shaped filter $\mu_{e,t}$ has been determined from minimizing $\overline{R_t^2}$, which given the assumption that $\mu_{e,t} = \mu_{e,r}$ is equal to $\overline{\langle R_r \rangle_r^2}$, while in case of the rectangular-shaped filter $\mu_{e,r}$ would have been determined from minimizing $\overline{R_r^2}$. The assumption that $\mu_{e,t} = \mu_{e,r}$ is only correct if the minimum of $\overline{R_r^2}$ is found at the same μ_e as the minimum of $\overline{\langle R_r \rangle_r^2}$. In general this will not be true, although the difference between the two effective viscosity estimates is expected to be small. Ideally, when the closure (9) would be exact and hence

$\overline{R_r^2} = \overline{\langle R_r \rangle_r^2} = 0$, the two viscosities would be the same. Indirect evidence that the effective viscosities are nearly the same for the two filters, was found from plotting figure 5.b for the case of the rectangular-shaped filter (not shown). From this figure it was observed that, just as for the triangular-shaped filter, $\overline{E^2}$ was significantly smaller over a large range of k when μ_e was given by (17) as compared to $\mu_e = \mu$.

References

[1] Brinkman, H. C. 1948 A calculation of the viscous force exerted by a flowing fluid on a dense swarm of particles. *Applied Scientific Research* **A1**, 27-34.

[2] Einstein, A. 1906 Eine neue Bestimmung der Moleküldimensionen. *Annalen der Physik* **19**, 289-306.

[3] Einstein, A. 1911 Berichtigung zu meiner Arbeit: "Eine neue Bestimmung der Moleküldimensionen.". *Annalen der Physik* **34**, 591-592.

[4] Lundgren, T. S. 1972 Slow flow through stationary random beds and suspensions of spheres. *J. Fluid Mech.* **51(2)**, 273-299.

[5] Freed, K. F., & Muthukumar, M. 1978 On the Stokes problem for a suspension of spheres at finite concentrations. *J. Chem. Phys.* **68(5)**, 2088-2096.

[6] Kim, S., & Russel, W. B. 1985 Modelling of porous media by renormalization of the Stokes equations. *J. Fluid Mech.* **154**, 269-286.

[7] Koplik, J., Levine, H., & Zee, A. 1983 Viscosity renormalization in the Brinkman equation. *Phys. Fluids* **26(10)**, 2864-2870.

[8] Martys, N., Bentz, D. P., & Garboczi, E. J. 1994 Computer simulation study of the effective viscosity in Brinkman's equation. *Phys. Fluids* **6(4)**, 1434-1439.

[9] Larson, R. E., & Higdon, J. J. L. 1986 Microscopic flow near the surface of two-dimensional porous media. Part 1. Axial flow. *J. Fluid Mech.* **166**, 449-472.

[10] Larson, R. E., & Higdon, J. J. L. 1987 Microscopic flow near the surface of two-dimensional porous media. Part 2. Transverse flow. *J. Fluid Mech.* **178**, 119-136.

[11] Kolodziej, J. A. 1988 Influence of the porosity of a porous medium on the effective viscosity in Brinkman's filtration equation. *Acta Mechanica* **75**, 241-254.

[12] Givler, R. C., & Altobelli, S. A. 1994 A determination of the effective viscosity for the Brinkman-Forchheimer flow model. *J. Fluid Mech.* **258**, 355-370.

[13] Bear, J. Dynamics of fluids in porous media. Dover Publications, New York, 1988.

[14] Breugem, W.-P., Boersma, B. J., & Uittenbogaard, R. E. 2004 Direct numerical simulations of plane channel flow over a 3D Cartesian grid of cubes. In *Proc. Intl Conf. on Applications of Porous Media* (ed. A. H. Reis & A. F. Miguel), pp. 27-34. Évora Geophysics Center, Évora, Portugal.

[15] Breugem, W.-P. The influence of wall permeability on laminar and turbulent flows. Theory and simulations. PhD thesis, Delft University of Technology, 2005. As of 2007, the thesis can be accessed at www.library.tudelft.nl/ws/search/publications/metadata/index.htm?docname=178423

[16] Quintard, M., & Whitaker, S. 1994 Transport in ordered and disordered porous media II: Generalized volume averaging. *Transport in Porous Media* **14**, 179-206.

[17] Gray, W. G. 1975 A derivation of the equations for multi-phase transport. *Chem. Eng. Sci.* **30**, 229-233.

[18] Breugem, W.-P., Boersma, B. J., & Uittenbogaard, R. E. 2006 The influence of wall permeability on turbulent channel flow. *J. Fluid Mech.* **562**, 35-72.

[19] Happel, J., & Brenner, H. Low Reynolds number hydrodynamics. Noordhoff International Publishing, Leyden, 1973.

[20] Wesseling, P. Principles of computational fluid dynamics. Springer-Verlag, Berlin, 2001.

[21] Lage, J.L. 1998 The fundamental theory of flow through permeable media from Darcy to turbulence. In *Transport Phenomena in Porous Media* (ed. D. B. Ingham & I. Pop), p. 1-30. Elsevier Science, Oxford, 1998.

[22] Chen, S., & Doolen, G. D. 1998 Lattice Boltzmann Method for fluid flows. *Annu. Rev. Fluid Mech.* **30**, 329-364.

[23] Mittal, R., & Iaccarino, G. 2005 Immersed boundary methods. *Annu. Rev. Fluid Mech.* **37**, 239-261.

[24] Breugem, W.-P., & Boersma, B. J. 2005 Direct Numerical Simulations of turbulent flow over a permeable wall using a direct and a continuum approach. *Phys. Fluids*, **17(2)**.

[25] Breugem, W.-P. 2006 An Immersed Boundary Method for flows around rectangular objects. In *Proc. European Conf. Computational Fluid Dyn. (ECCOMAS CFD)* (ed. P. Wesseling, E. Oñate & J. Périaux). TUDelft, Netherlands, 2006.